DOI: http://dx.doi.org/10.1590/2179-10742017v16i1738

Design of a Compact UWB Bandpass Filter using Via-Less CRLH TL

[1]Dileep Kumar Upadhyay, [2]Uday Kumar, [3]Gajendra Kant Mishra
[1,2,3]Department of Electronics and Communication Engineering, Birla Institute of Technology, Mesra,Ranchi, India
Emails: [1]dileep_bit@yahoo.com
[2]ranjanuday333@gmail.com
[3]gkmishra@bitmesra.ac.in
[4]Babu Lal Shahu
[4]Department of Electronics and Communication Engineering, Birla Institute of Technology, Mesra, Deoghar Campus, Deoghar-814142, India
Email:[4]sahu.babulal@gmail.com

***Abstract*— A novel compact ultra wideband (UWB) bandpass filter (BPF) based on composite right/left handed transmission line (CRLH TL) is reported in this paper. The proposed UWB BPF is designed and developed by coupling of two unit-cells of via-less CRLH TL, excited by asymmetrical coplanar waveguide (CPW) feed-line. The unit cell of CRLH TL is designed using series interdigital capacitor (IDC) in shunt with the shorted inductive stub. Because of the CPW-fed, no via is required to get the shunt inductance for the realization of CRLH TL, which minimizes the fabrication steps. The filter is compact in size 11.9 x 6 mm^2. The proposed filter exhibits the return-loss ($|S_{11}|$) more than 11.2 dB and insertion-loss ($|S_{21}|$) less than 0.5 dB and low and flat group delay response throughout the passband, 3.3 GHz to 13.0 GHz. The proposed UWB BPF also shows the good stopband rejection ($|S_{21}|$ > 20 dB and $|S_{11}|$ < 0.8 dB) from 13.6 GHz to 15 GHz and steep roll-off from passband to stopband. The fractional bandwidth (FBW) of the filter is found to be 119 %. The equivalent lumped circuit model of the filter is obtained through Ansoft Designer. All simulated results are extracted through method of moment based simulator, IE3D. Agilent vector network analyzer (VNA) is used to get the measured results. All measured results are found in close similarity with the simulated results.**

***Index Terms*—** Composite right/left handed transmission line, Interdigital capacitor, Ultra wideband bandpass filter.

I. INTRODUCTION

The left handed metamaterials can be realized mainly by two methods, firstly, using periodic arrangement of split ring resonators and thin metallic wires and, secondly by dual of conventional right handed transmission line, i.e. by periodic arrangement of series interdigital capacitors in shunt with the shorted stubs to ground. The first and second methods are respectively known as resonant and non-resonant approach of realization of left handed metamaterials. Due to large in size and lossy in nature, the resonant approach is not well suited for the realization of left handed metamaterials [1]. Since 2002 the U.S. Federal Communications Commission (FCC) [2] has regularized the unlicensed use of UWB frequency band 31. GHz to 10.6 GHz, the research in the field of UWB bandpass filter

Brazilian Microwave and Optoelectronics Society-SBMO *received 08 Sep 2016; for review 08 Seo 2016; accepted 12 Jan 2017*
Brazilian Society of Electromagnetism-SBMag *© 2017 SBMO/SBMag* *ISSN 2179-1074*

DOI: http://dx.doi.org/10.1590/2179-10742017v16i1738

has gained much attention and challenges. The design of ultra wideband components need much efforts and attentions as it requires the good selectivity, low insertion-loss and low and constant group delay throughout the passband.

The UWB BPF reported in [3] is based on conventional CRLH TL designed by using via. The reported UWB BPF in [3] has good S-parameters characteristics and compact in size (16.4 x 4.8 mm^2). Moreover because of the use of via it requires the extra fabrication processing steps for drilling and soldering as compared to the proposed UWB BPF. The UWB bandpass filter presented in [4] is based on defected ground structure (DGS) as split ring resonator and conventional CRLH TL with via. The reported filter [4] is compact in size, 13 x 8.5 mm^2, however because of the split ring resonator structure in ground plane and the presence on via, it requires the more extra efforts in ground plane processing and for creation of via. A single CRLH TL cell based UWB band pass filter [5] operating over the frequency band of 4 GHz to 9.5 GHz is of relatively large in size, 30 x 8.5 mm^2 and also requires the via for the realization of CRLH TL. The reported filter [5] also suffers with the poor S-parameters performance in passband ($|S_{21}|$ = 1.5 dB) as well as in stopband. A compact UWB band pass filter (18.4 x 4.5 mm^2) reported in [6] has good S-parameters performance ($|S_{21}|$ < 0.3 dB and $|S_{11}|$ > 10 dB) is designed on via-less CRLH TL. Moreover the reported UWB BPF [6] operated over relatively low frequency band 3.1 GHz to 10.6 GHz and relatively large in size as compared to the proposed UWB BPF (frequency band, 3.3 GHz to 13.0 GHz and size, 11.9 x 6 mm^2). An ultra wideband band pass filter designed using interdigitated coupled lines CRLHTL structure [7] operated over 3.9 GHz to 10.3 GHz is relatively large in size (30 x 15 mm^2), requires the generation of via and suffers with relatively poor insertion loss ($|S_{21}|$ = 1.5 dB).

Many researchers and scientists worldwide have investigated, designed and developed various UWB BPFs based on different techniques such as; by use of fractal geometry, defected ground plane, coupled line structure and multimode resonator etc. References [8-13] report the various UWB BPFs based on different techniques such as a CRLH TL and fractal geometry based UWB BPF [8], the coupled structure based ultra wideband bandpass filter [9], defected ground structure [10], modified CRLH TL with cross coupling [11], cascading bandpass and bandstop filters [12] and multi mode resonator based UWB BPF [13]. The UWB BPFs [8-13] designed using different techniques are considered in this paper for comparison of various parameters with the proposed UWB BPF.

In this paper design and development of a compact (11.9 x 6 mm^2) ultra wideband bandpass filter based on via-less CRLH TL is reported. Since in CPW-fed, the signal plate and ground plate both reside on the top plane of the dielectric substrate, hence no via is required for the realization of proposed CRLH TL, in contrast to conventional design of CRLH TL, where, via is required to short circuit the shunt inductive stub to ground. The absence of via reduces the fabrication steps, saves the valuable time wastage and minimizes the overall bulk production cost. The proposed UWB BPF is designed by coupling between two similar unit-cells of CRLH TL. The unit-cell of CRLH TL is designed by series five fingers based interdigital capacitor in shunt with the inductive stub shorted to

 © 2017 SBMO/SBMag *ISSN 2179-1074*

DOI: http://dx.doi.org/10.1590/2179-10742017v16i1738

the one of the ground plane of CPW feed-line. The filter exhibits the return-loss greater than 11.2 dB and insertion-loss less than 0.5 dB to whole passband frequency range, 3.3 GHz to 13 GHz, with steep roll-off during the transition from stopband to passband and stopband rejection level greater than 20 dB for frequency range of 13.3 GHz to 15 GHz. The filter shows the low (maximum variation of 0.8 ns) and constant group delay throughout the passband. The proposed UWB BPF is designed and developed on RT/duroid dielectric substrate with relative permittivity of 2.2, thickness of 1.57 mm and loss-tangent of 0.0009. The equivalent lumped circuit model of the proposed filter is obtained using circuit model tool of Ansoft Designer. The simulation and measured results are obtained from electromagnetic (EM) simulator, IE3D and vector network analyzer respectively. All measured results are found in close similarity with the simulated results.

II. THEORY AND DESIGN OF PROPOSED UWB BANDPASS FILTER

The composite right/left handed transmission line can be realized by dual of conventional right handed transmission line (RH TL), known as non-resonant approach. The pure right handed transmission line (PRH TL) consists of series inductor in shunt with the capacitor, whereas pure left handed transmission line (PLH TL) is realized by series capacitor in shunt with the inductor. Unfortunately, either PRH TL or PLH TL cannot be physically realized because of the unavoidable parasitic effects of microstrip transmission lines. Hence because of the unavoidable parasitic effects, the CRLH TL is realized rather than the PRH TL. The CRLH TL shows the virtue of both, the nature of left handed transmission line (LH TL) at low frequencies and the nature of RH TL at high frequencies [1].

The unit-cell of CRLH TL consists of per-unit series LH capacitance (C_{LH}) and per-unit right handed inductance (L_{RH}) and per-unit shunt LH inductance (L_{LH}) and per-unit RH capacitance (C_{RH}). The combination of series RH inductance (L_{RH}) and shunt RH capacitance (C_{RH}) in CRLH TL works as a lowpass filter whose cut-off frequency is given as $f_{CR} = \frac{1}{2\pi\sqrt{L_{RH}C_{RH}}}$. The combination of series LH capacitance (C_{LH}) and shunt LH inductance (L_{LH}) in CRLH TL works as a highpass filter whose cut-off frequency is given as $f_{CL} = \frac{1}{2\pi\sqrt{L_{LH}C_{LH}}}$. So, when $f_{CR} < f_{CL}$, the CRLH TL works as a wideband bandpass filter.

The series, f_{SE} and shunt, f_{SH} resonance frequencies of the CRLH TL are given as follows

$$f_{SE} = \frac{1}{2\pi\sqrt{L_{RH}C_{LH}}} \tag{1}$$

$$f_{SH} = \frac{1}{2\pi\sqrt{L_{LH}C_{RH}}} \tag{2}$$

For balanced CRLH TL,

$$f_{SE} = f_{SH} = f_C = \sqrt{f_{SE}\, f_{SH}} \tag{3}$$

Brazilian Microwave and Optoelectronics Society-SBMO *received 08 Sep 2016; for review 08 Seo 2016; accepted 12 Jan 2017*
Brazilian Society of Electromagnetism-SBMag *© 2017 SBMO/SBMag* *ISSN 2179-1074*

DOI: http://dx.doi.org/10.1590/2179-10742017v16i1738

Where, f_C is known as centre frequency. The lower end, f_L and upper end, f_U frequencies of CRLH TL are given as follows

$$f_L = \frac{1}{2\pi\sqrt{L_{RH}C_{LH}}} \tag{4}$$

$$f_U = \frac{1}{2\pi\sqrt{L_{RH}C_{LH}}} \tag{5}$$

The design layout of proposed ultra wideband bandpass filter with the notation of all physical dimensions is depicted in Fig.1. The filter is excited by asymmetrical CPW-fed, which consists of two ground planes. As shown in Fig. 1, UWB BPF is designed using coupling of two symmetrical series interdigital capacitors (IDC). The IDC consists of five fingers of finger length L_3, finger width S_2 and finger spacing S_1. The coupling gap between the two IDCs is S_6. The two stubs each of length L_9, is connected to each IDC and ground plane 2 to get the shunt inductance. Since signal plane and ground plane both are in same planes, hence no via is required to short circuit the stubs to ground plane 2, in contrast to the conventional method of design of CRLH TL with via. The absence of via minimizes the fabrication steps, saves the fabrication time and reduces the overall bulk production cost. The filter is compact in size, 11.9 x 6 mm^2.

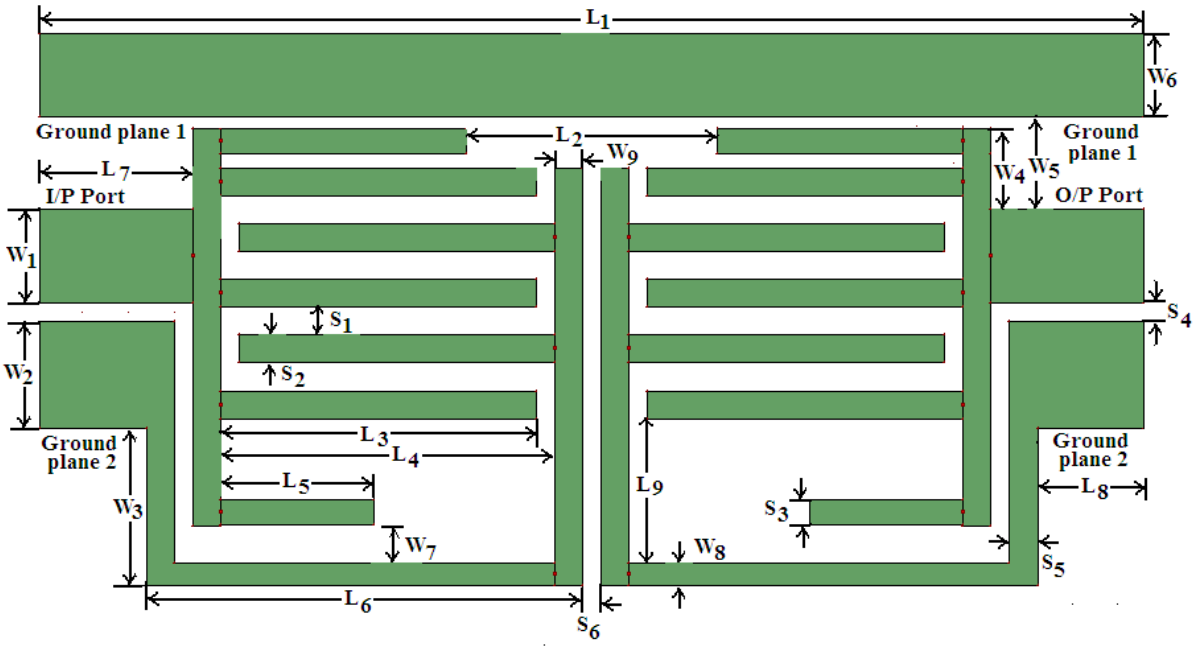

Fig. 1. Design layout of the proposed ultra wideband bandpass filter

III. EFFECTS OF VARIATION OF VARIOUS PHYSICAL PARAMETERS ON UWB BPF

All optimized physical dimensions of the proposed UWB BPF are obtained by parametric study of the geometry shown in Fig.1. The nature of variation of S-parameters characteristics of filter is investigated and analyzed for variation on one physical parameter keeping other parameters constant, to get the best optimized physical dimensions of the geometry, which can meet the low insertion-loss and return-loss better than 10 dB throughout the passband.

© 2017 SBMO/SBMag

DOI: http://dx.doi.org/10.1590/2179-10742017v16i1738

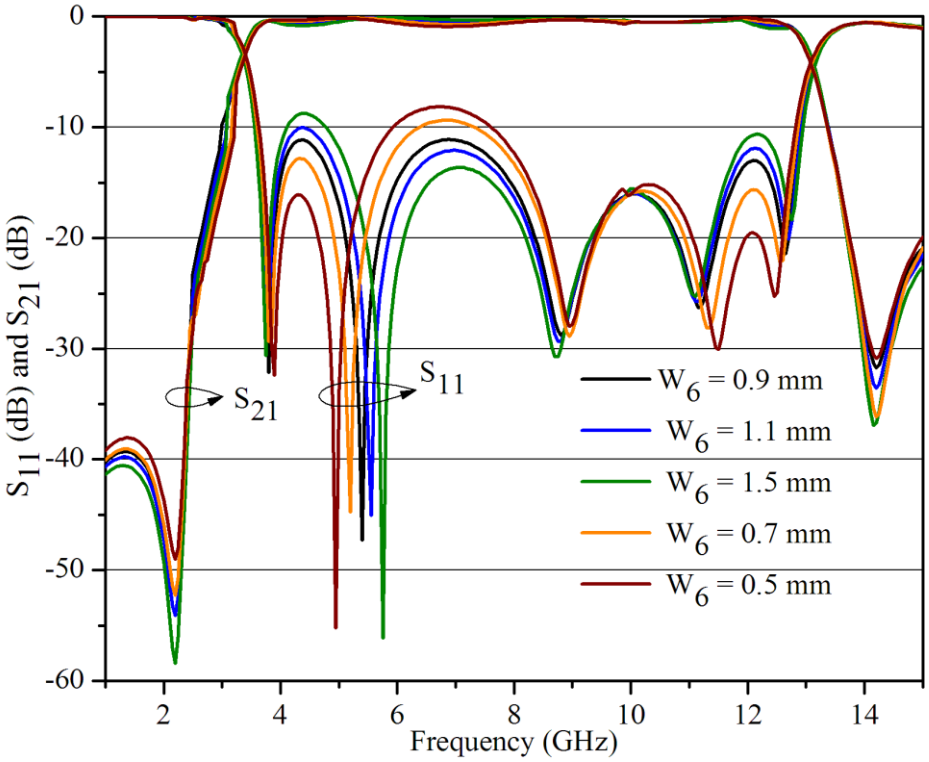

Fig. 2. S-parameters vs. Frequency plot for the variation of parameter W_6

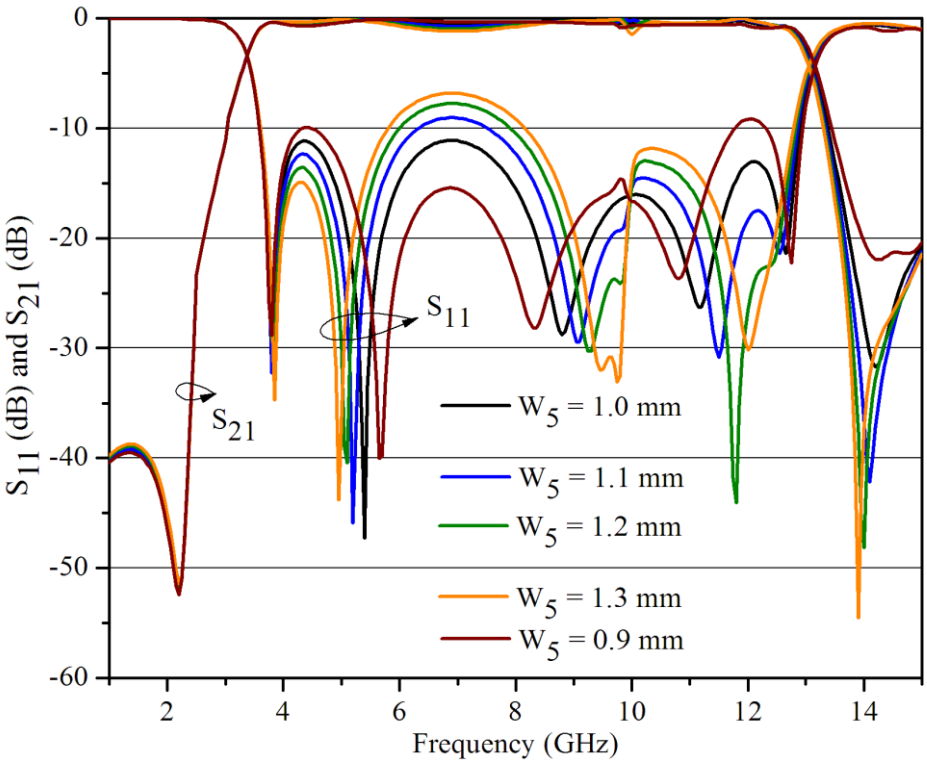

Fig. 3. S-parameters vs. Frequency plot for the variation of parameter W_5

The effects of variation of physical parameter W_6 is shown in Fig. 2. The optimum value of W_6 is taken to be 0.9 mm. It can be seen from Fig. 2 that as the value of W_6 is increased from 0.9 mm to 1.5 mm, the S-parameters improve in frequency band 6.0 GHz to 8.0 GHz and deteriorate in the frequency band of 4 GHz to 4.8 GHz and 11.7 GHz to 12.4 GHz for the constant bandwidth 3.3 GHz

 © 2017 SBMO/SBMag *ISSN 2179-1074*

DOI: http://dx.doi.org/10.1590/2179-10742017v16i1738

to 13.0 GHz. As the value of W_6 is decreased from 0.9 mm to 0.5 mm, the value of S-parameters deteriorate in frequency band 6.0 GHz to 8.0 GHz and improve in 4 GHz to 4.8 GHz and 11.7 GHz to 12.4 GHz. So the value of W_6 is considered as 0.9 mm by compromising the performance in passband. The sensitivity for the variation of physical parameter, W_5 on S-parameters versus frequency plot is shown in Fig. 3. As the value of W_5 increases from 1.0 mm to 1.3 mm, the S-parameters performance deteriorate in frequency band 6.0 GHz to 8.0 GHz and improve in the frequency band 4 GHz to 4.8 GHz. The vice-versa effects can be seen for the value of W_5 less than 1.0 mm. Hence the optimized value of W_5 is chosen to be 1.0 mm, by considering the performance of S-parameters in both bands. For the variation of W_5, the overall bandwidth remains almost constant, i.e. from 3.3 GHz to 13.0 GHz. The effects of variation of physical parameters L_2 on S-parameters versus frequency plot is depicted in Fig. 4. Considering the response of S-parameters in the band 4.0 GHz to 8.0 GHz and 11.7 GHz to 12.4 GHz, the optimum value of L_2 is considered as 2.7 mm.

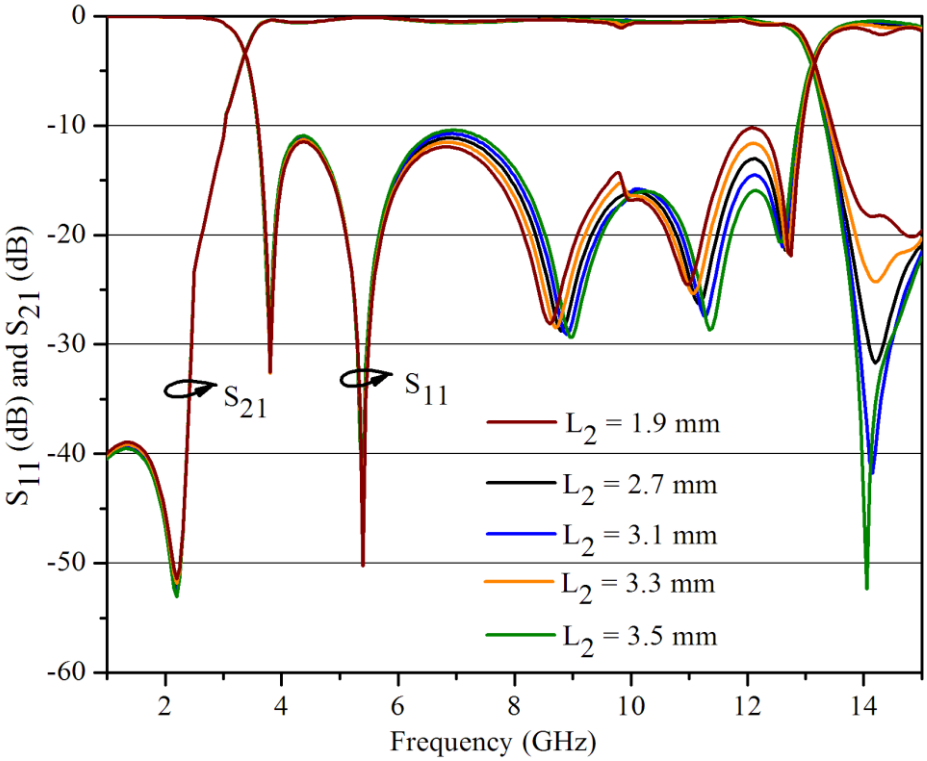

Fig. 4. S-parameters vs. Frequency plot for the variation of parameter L_2

The sensitivity for the variation of physical parameter L_9 on S-parameters response is shown in Fig. 5. The optimized value of L_9 is considered to be 1.6 mm. As the value of L_9 increases from 1.6 mm to 2.2 mm, the S-parameters performance deteriorate in the frequency bands 6.0 GHz to 8.0 GHz and 4.0 GHz to 4.8 GHz and improve in the frequency bands 9.0 GHz to 11.0 GHz and 11.7 GHz to 12.4 GHz. For the value of L_9 less than 1.6 mm, the vice-versa effects are observed in all considered bands. The S-parameters versus frequency plot for the variation of physical parameter L_5 is shown in Fig. 6. Considering the performance of S-parameter throughout the passband, the value of L_5 is chosen to be 1.65 mm. As the value of L_5 increases 1.65 mm to 2.25 mm, the high end frequency

 © 2017 SBMO/SBMag *ISSN 2179-1074*

DOI: http://dx.doi.org/10.1590/2179-10742017v16i1738

shifted from 13.0 GHz to 12.5 GHz and S-parameters deteriorate in the frequency band 11.7 GHz to 12.4 GHz. For the lower values of L_5, the high end frequency shifted from 13.0 GHz to 13.5 GHz, but S-parameters response slightly deteriorate in frequency bands 6.0 GHz to 8.0 GHz and 4.0 GHz to 4.8 GHz.

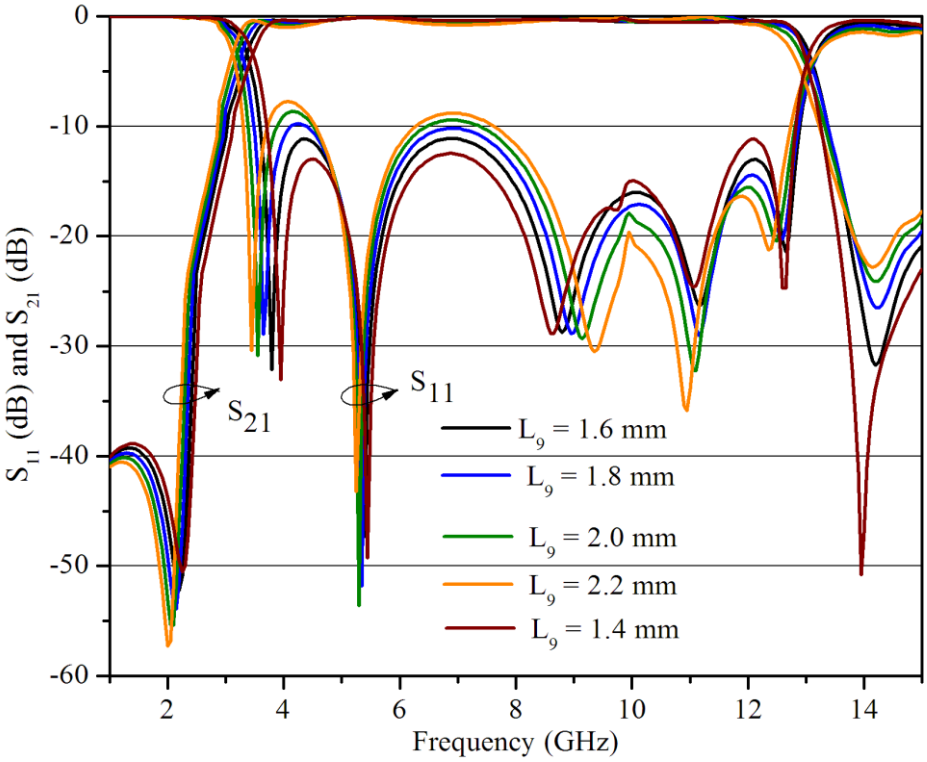

Fig. 5. S-parameters vs. Frequency plot for the variation of parameter L_9

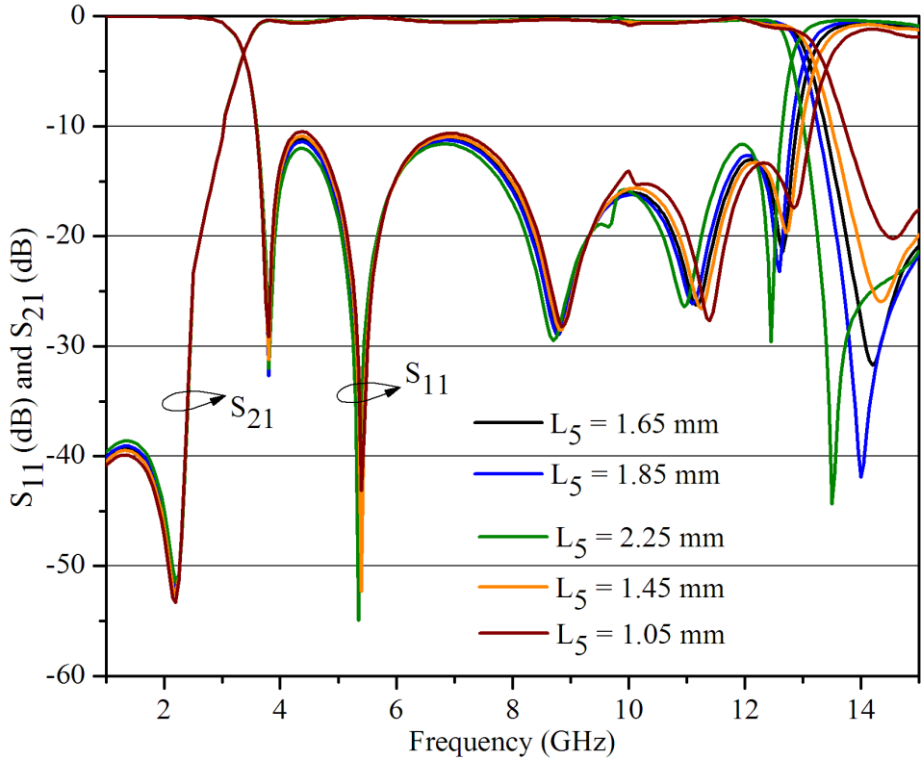

Fig. 6. S-parameters vs. Frequency plot for the variation of parameter L_5

received 08 Sep 2016; for review 08 Seo 2016; accepted 12 Jan 2017
© 2017 SBMO/SBMag
ISSN 2179-1074

DOI: http://dx.doi.org/10.1590/2179-10742017v16i1738

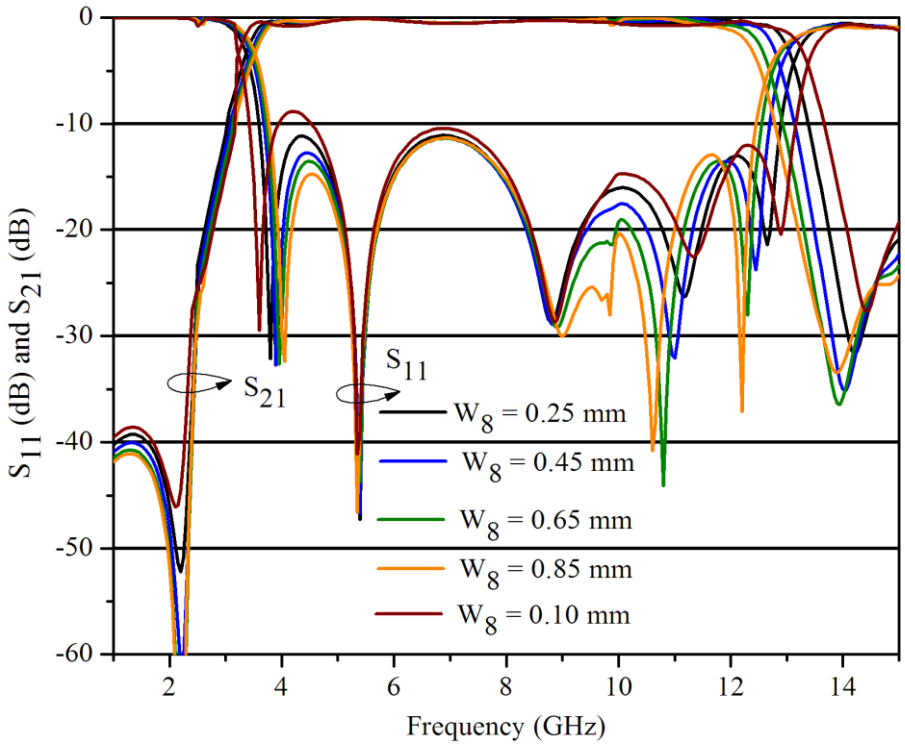

Fig. 7. S-parameters vs. Frequency plot for the variation of parameter W_8

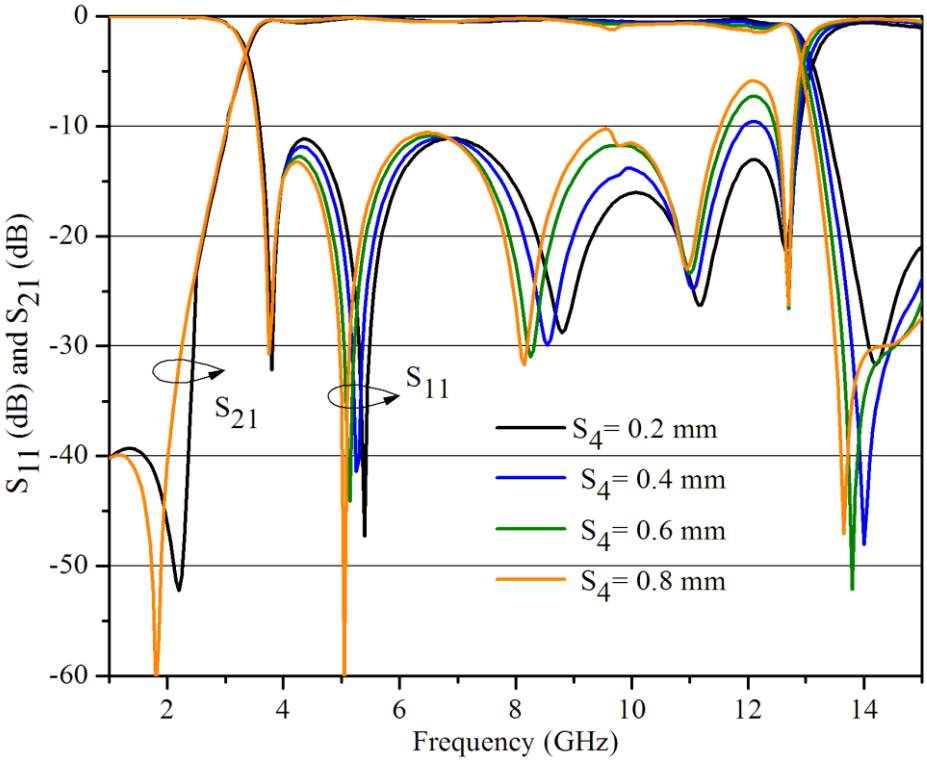

Fig. 8. S-parameters vs. Frequency plot for the variation of parameter S_4

The effects on S-parameters response for the change of width of ground plane 2, W_8 is illustrated in Fig. 7. The optimum value of W_8 is considered as 0.25 mm. From the Fig. 7, it can be observed that by increasing the value of W_8 from 0.25 mm to 0.85 mm, the S-parameters improve in passband but at the same time the high end frequency decreases from 13 GHz for the case of W_8 = 0.25 mm to 12.4

 © 2017 SBMO/SBMag *ISSN 2179-1074*

DOI: http://dx.doi.org/10.1590/2179-10742017v16i1738

GHz for the case of W_8 = 0.85 mm. The shift in high end frequency to the lower end, decreases the overall bandwidth, which is not desirable. Decreasing the value of W_8 from 0.25 mm to 0.1 mm the overall bandwidth increases, but the passband S-parameters performance become poor. The effect on S-parameters response for the variation of physical parameter S_4, is depicted in Fig. 8. Changing the value of S_4, the overall bandwidth remains almost unchanged. By increasing the value of S_4 from 0.2 mm to 0.8 mm, the S-parameters performance of the filter deteriorates in passband. Hence, the optimum value of S_4 is chosen to be 0.2 mm. The effects of variation of the coupling gap S_6, between the two interdigital capacitors on S-parameters performance is illustrated in Fig. 9. Increasing the value of S_6 from 0.2 mm to 0.8 mm, the S-parameters performance and overall bandwidth of the filter remain almost invariant. For zero gap between the two interdigital capacitors (S_6 = 0.0 mm), the return-loss and insertion-loss deteriorate by considerable amount. Hence, an optimum value of S_6 is considered as S_6 = 0.2 mm. For others value of physical parameters, similar parametric studies discussed for Fig. 2 to Fig. 9 are performed and their optimum values are found. Similar to parametric studies performed and depicted from Fig. 2 to Fig. 9. The various optimized physical dimensions of the proposed UWB BPF is listed in Table I.

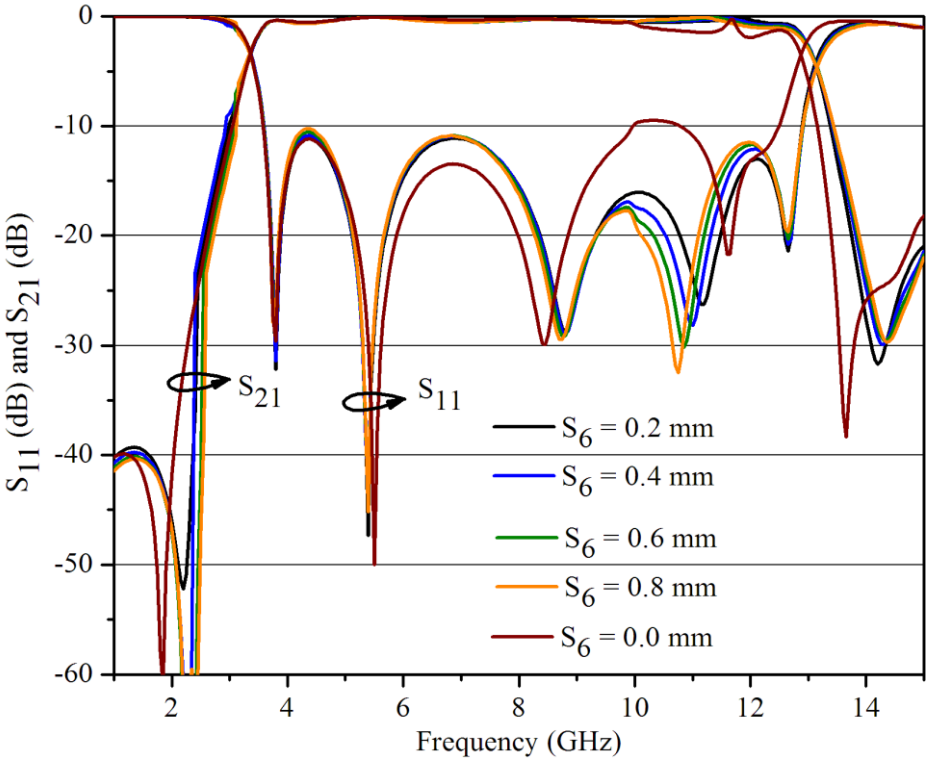

Fig. 9. S-parameters vs. Frequency plot for the variation of parameter S_6

© 2017 SBMO/SBMag

DOI: http://dx.doi.org/10.1590/2179-10742017v16i1738

TABLE I. OPTIMIZED PHYSICAL PARAMETERS OF PROPOSED UWB BPF SHOWN IN FIG. 1

Parameter	L_1	L_2	L_3	L_4	L_5	L_6	L_7	L_8
Dimension (mm)	11.9	2.7	3.4	3.6	1.65	4.7	1.65	1.15
Parameter	L_9	W_1	W_2	W_3	W_4	W_5	W_6	W_7
Dimension (mm)	1.6	1.0	1.15	1.7	0.87	1.0	0.9	0.4
Parameter	W_8	W_9	S_1	S_2	S_3	S_4	S_5	S_6
Dimension (mm)	0.25	0.3	0.3	0.3	0.27	0.2	0.3	0.2

IV. EQUIVALENT LUMPED CIRCUIT MODEL ANALYSIS

The equivalent lumped circuit mode of the proposed UWB BPF shown in Fig. 1 is depicted in Fig. 10. The equivalent lumped circuit model results are obtained using circuit model tool of the Ansoft Designer. Considering the layout of the proposed UWB BPF, an equivalent circuit diagram is designed. The lumped element values are manually optimized by changing the each element value so that it can have the good agreement with the simulated results obtained from the full wave simulator. In the lumped equivalent circuit diagram, the mutual coupling between the individual elements is not taken in to consideration. The inductive components, L_1 and L_2 are generated because of the input and output CPW-fed transmission lines. The left handed capacitors, C_{LH1} and C_{LH2} are introduced because of the input and output interdigital capacitors. The right handed inductances, L_{RH1} and L_{RH2} are included because of the parasitic effects in input and output IDCs. The shunt left handed inductances L_{LH11}, L_{LH12}, L_{LH21} and L_{LH22} are generated because of the input and output stubs shorted to the ground plane 2. The shunt right handed capacitances C_{RH11}, C_{RH12}, C_{RH21} and C_{RH22} are introduced due to the

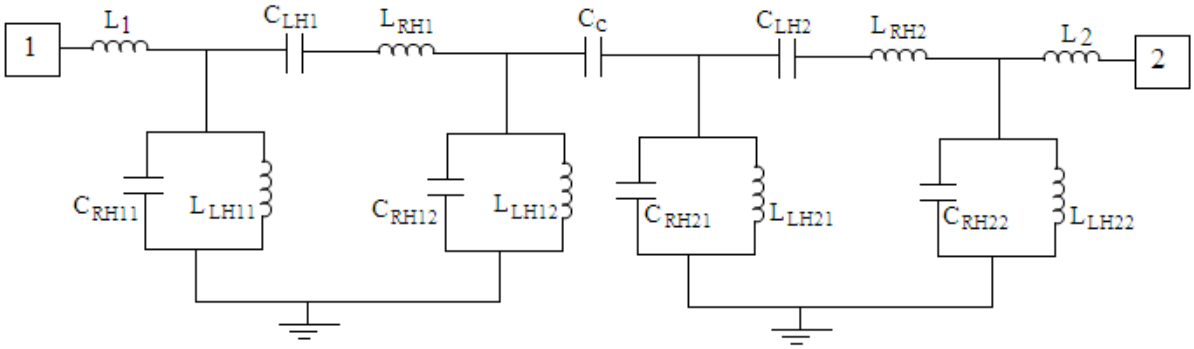

Fig. 10. Equivalent lumped circuit model of the proposed UWB BPF shown in Fig. 1

TABLE II. COMPONENTS VALUES OF THE EQUIVALENT LUMPED CIRCUIT MODEL SHOWN IN FIG. 10

Component	L_1	L_2	L_{RH1}	L_{RH2}
Value (nH)	0.1	0.3	1.25	1.24
Component	L_{LH11}	L_{LH12}	L_{LH21}	L_{LH22}
Value (nH)	1.25	1.1	1.7	1.3
Component	C_{LH1}	C_{LH2}	C_{RH11}	C_{RH12}
Value (pF)	0.5	0.55	0.5	9.45
Component	C_{RH21}	C_{RH22}	C_C	
Value (pF)	0.3	0.55	1.4	

© 2017 SBMO/SBMag

DOI: http://dx.doi.org/10.1590/2179-10742017v16i1738

parasitic effects of shorted stubs to ground plane 2 and the gap ($W_5 - W_4$) between topmost additional finger of IDC to the ground plane 1. The various components values of the equivalent lumped circuit model shown in Fig. 10 are listed in Table II.

The comparative S-parameters versus frequency response of EM simulation and circuit model are illustrated in Fig. 11. The EM simulation results are taken corresponding to the optimized physical parameters listed in Table I. The close similarity between the EM simulation and circuit model results are observed, however a slight deviation between the two may be seen which may arise because of the ignorance of mutual coupling between the individual circuit elements. The -3.0 dB insertion-loss frequency bands for EM simulation and circuit model are found to be 3.3 GHz to 13.0 GHz and 3.2 GHz to 13.1 GHz respectively. The passband insertion-loss is less than 0.5 dB and 0.25 dB respectively and reflection-loss greater than 11.2 dB and 10.9 dB respectively for EM simulation and circuit model. The EM simulation results show the good stopband rejection ($|S_{21}| > 20$ dB and $|S_{11}| < 0.8$ dB) from 13.6 GHz to 15 GHz and steep roll-off from passband to stopband. The fractional bandwidth of the filter is found to be 119 %.

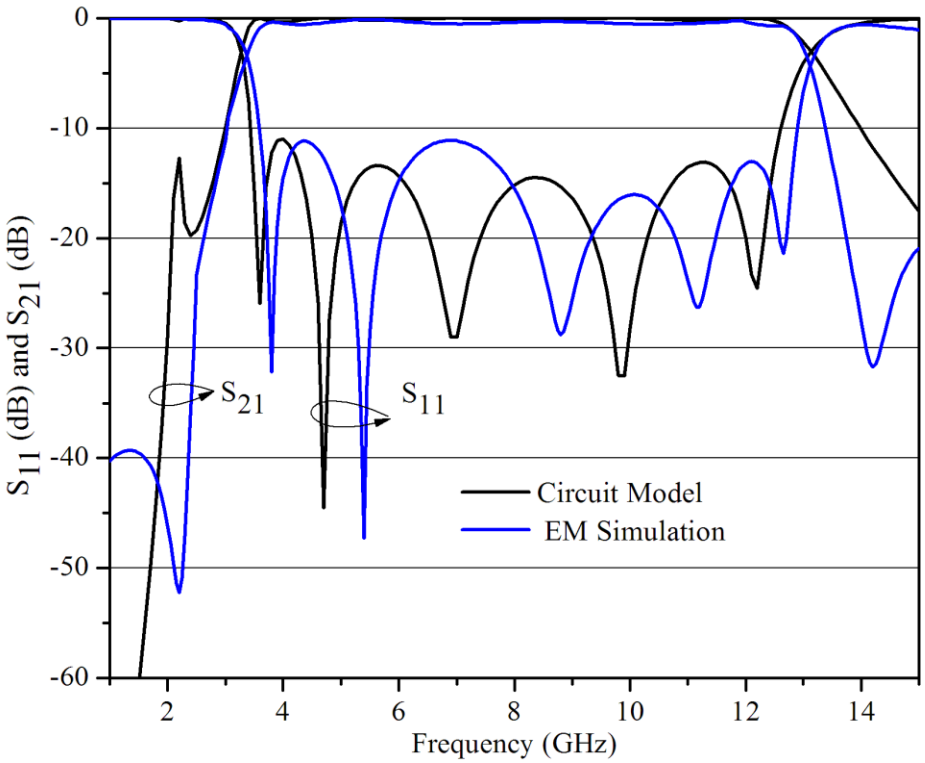

Fig. 11. Comparative S-parameters vs. Frequency plot of equivalent circuit model and EM simulation

V. MEASUREMENT RESULTS AND DISCUSSION

Based on the optimized physical parameters listed in Table I, the proposed UWB BPF shown in Fig.1 is fabricated and its performance parameters are measured using Agilent vector network analyzer. Fig. 12 shows the photograph of fabricated prototype of proposed UWB BPF. The comparative simulated and measured S-parameters versus frequency response are shown in Fig. 13. From the Fig. 13, a close similarity between the simulated and measured results can be observed.

 © 2017 SBMO/SBMag *ISSN 2179-1074*

DOI: http://dx.doi.org/10.1590/2179-10742017v16i1738

Moreover a little deviation between the simulated and measured results can be seen, which mainly arise because of the finite ground plane, improper soldering and fabrication tolerances. The measured -3.0 dB insertion-loss frequency band of the proposed UWB BPF is found to be 3.12 GHz to 12.43 GHz, whereas the simulated -3.0 dB insertion-loss frequency band is found to be 3.3 GHz to 13.0 GHz. In throughout the passband, the measured and simulated insertion-losses are less than 0.6 dB and 0.5 dB respectively, whereas return-losses are more than 10.4 dB and 11.2 dB respectively. The mesured fractional bandwidth of the filter is found to be 120 %.

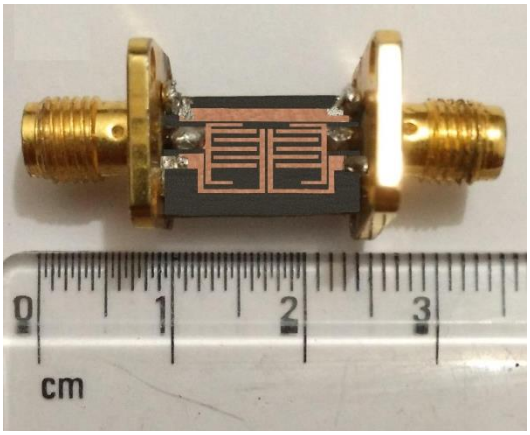

Fig. 12. Prototype of fabricated proposed UWB BPF

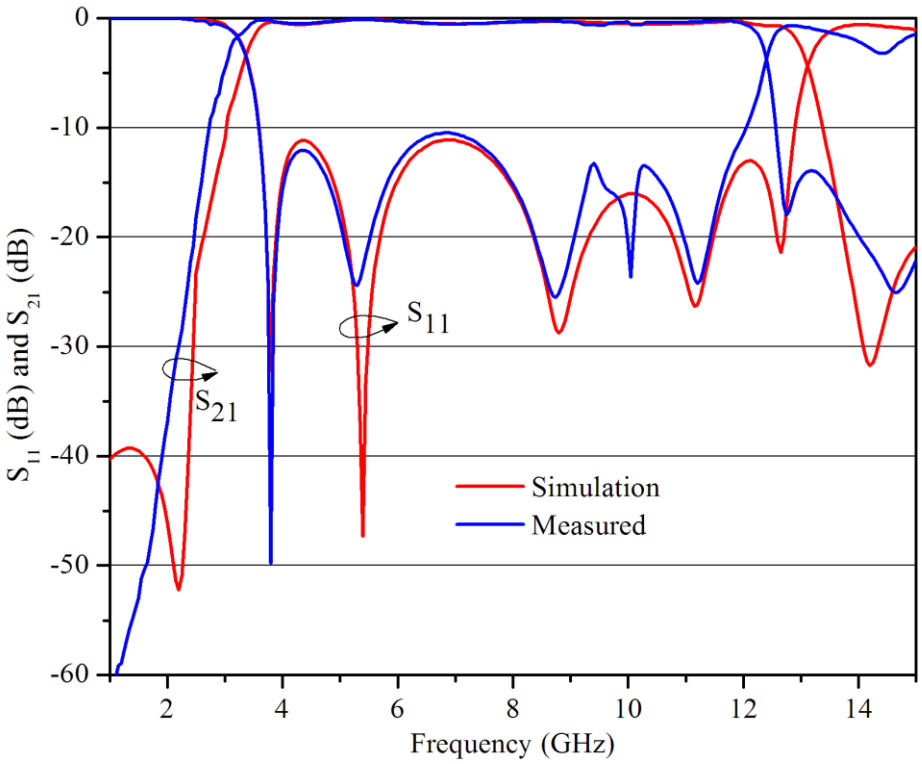

Fig. 13. Comparative simulated and measured S-parameters vs. Frequency plot

The simulated and measured group delay versus frequency response of the proposed ultra wideband bandpass filter is depicted in Fig. 14. The low and constant group delay response can be observed throughout the passband of UWB BPF. The simulation and measured group delay vary between the 0.7 ns to 1.5 ns and 0.76 ns to 1.74 ns respectively, hence the maximum variation of simulated and

 © 2017 SBMO/SBMag *ISSN 2179-1074*

DOI: http://dx.doi.org/10.1590/2179-10742017v16i1738

measured group delays are 0.80 ns and 0.98 ns respectively. However, relatively large variation of group delays in both, simulation and measured results may be observed at both ends of the passband, which arises because of the sharp transition of insertion-loss curve from passband to stopband. The large difference between the simulated and experimental results at frequency 2.6 GHz may be seen because of the fabrication tolerances and improper soldering during the development of the UWB BPF.The low and flat group delay response throughout the operating passband frequency band shows the good time domain response of the filter. Comparative EM simulated, equivalent lumped circuit model and measured performance of the proposed UWB BPF are listed in Table III. The physical parameters, fabrication complexities and performance of the proposed UWB BPF are compared in Table IV with the ealrier reported UWB BPFs.

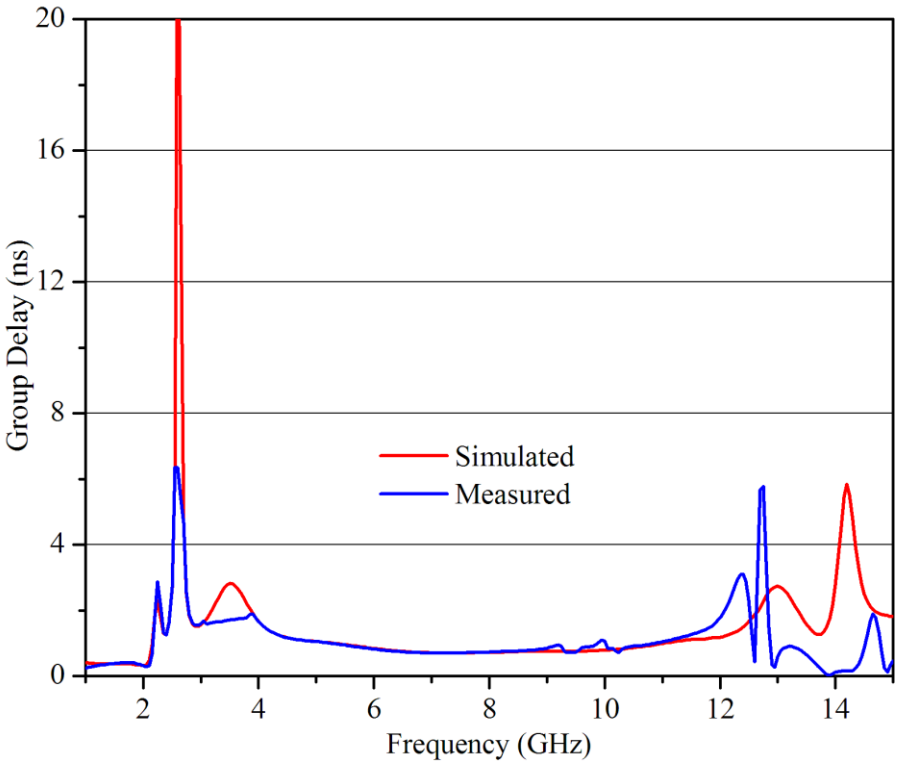

Fig. 14. Comparative simulated and measured group delay vs. Frequency plot

TABLE III. COMPARISON OF EM SIMULATION, CIRCUIT MODEL AND MEASURED RESULTS

Parameters	$\|S_{11}\|$ dB	$\|S_{21}\|$ dB	Frequency range (GHz)	Bandwidth (GHz)	FBW (%)	Group delay (ns)
Simulated	11.2	0.5	3.3 – 13.0	9.7	119	0.80
Circuit Model	10.9	0.25	3.2 – 13.1	9.9	121	--
Measured	10.4	0.6	3.12 – 12.43	9.31	120	0.98

© 2017 SBMO/SBMag

DOI: http://dx.doi.org/10.1590/2179-10742017v16i1738

TABLE IV. COMPARISON OF PROPOSED UWB BPF WITH THE VARIOUS REPORTED UWB BPF

Ref.	$\|S_{21}\|$ (dB)	$\|S_{11}\|$ (dB)	Frequency Range (GHz)	Size (mm)	Area (mm^2)	Via
[3]	0.5	11	2.9-10.75	16.8 x 4.8	80.64	Yes
[4]	1.0	13	3.1-10.6	13 x 8.5	110.5	Yes
[5]	1.0	10	4.0-9.5	30 x 8.5	255	Yes
[6]	0.3	10	3.15-10.8	18.4 x 4.5	82.8	No
[7]	1.5	10	3.9-10.3	30 x 15	450	Yes
[8]	1.1	15.2	2.5-11	30 x 20	600	No
[9]	1.0	14	2.8-10.9	30 x 20	600	Yes
[10]	2.5	15	0 - 18	26.2 x11.9	311.78	No
[11]	1.35	13	3.1 – 10.6	13 x 7.8	101.4	Yes
[12]	1.0	13	2.96 -10.43	42.3 x 12.3	520.3	Yes
[13]	0.68	17	3.4 – 10.7	21 x 5.3	111.3	Yes
This work	0.6	10.4	3.12 – 12.43	11.9 x 6	71.4	No

VI. CONCLUSION

Design and development of a compact CRLH TL based UWB BPF is presented in this paper. The CRLH TL is designed on coupling of two unit-cells of via-less CRLH TL. The filter is compact in size 11.9 x 6 mm^2 and excited by the CPW-fed. Due of the absence of via the filter ease the fabrication process and saves the time taken to build the vias. The developed UWB BPF shows the measured insertion-loss less than 0.6 dB and return-loss more than 10.4 dB throughout the passband 3.12 GHz – 12.43 GHz with fraction bandwidth of 120 %. Moreover, filter also shows the low (maximum deviation of 0.98 ns) and flat group delay response throughout the passband. Because of the compact in size and good in performance the proposed UWB BPF may find the potential applications in modern small sized wireless communication systems.

REFERENCES

[1] A. Lai, C. Caloz, and T. Itoh, "Composite right/left-handed transmission line metamaterials," *IEEE Microwave Mag. 5*, vol. 5, pp. 34–50, 2004.

[2] Revision of Part 15 of the commission's rules regarding ultra- wideband transmission system,*"ET-Docket 98-153, First note and order, Federal Communication Commission,"* Feb 2002.

[3] K.U. Ahmed and B.S. Virdee, *"Ultra-wideband bandpass filter based on composite right/left handed transmission-line unit-cell,"* IEEE Trans Microwave Theory Tech, vol. 61, pp. 782-788, 2013.

[4] A. Alburaikan, M. Aqeeli, X. Huang, and Z. Hu, *"Miniaturized ultra-wideband bandpass filter based on CRLH-TL unit cell," In: Microwave Conference (EuMC), Rome, Italy*, pp. 540–543, 2014.

[5] Fitri Yuli Zulkifli, Andik Atmaja and Eko Tjipto Rahardjo, "Implementation of single cell composite right–left handed transmission line for ultra wideband bandpass filter," *International Journal of Technology (IJTech)*, vol. 2, pp. 121-128, 2012.

[6] Nilotpal and Dileep Kumar Upadhyay, "A compact UWB bandpass filter based on CRLH via-less CPW-fed," *Microwave and Optical Technology Lett*, vol. 58, pp. 276-279, 2016.

[7] B. Qian, D. Jun, and G. Chen Jiang, "New design of ultra wideband filter using interdigitated coupled lines CRLHTL structure," *In: 2012 10th International Symposium on Antennas, Propagation & EM Theory (ISAPE), Xian, China*, pp. 486–489, 2012

 © 2017 SBMO/SBMag

DOI: http://dx.doi.org/10.1590/2179-10742017v16i1738

[8] Xu, H.-X., Wang, G.-M., and Zhang, C.-X., "Fractal-shaped UWB bandpass filter based on composite right/left handed transmission line," *Elect. Lett.*, vol. 46, no.4, pp. 285-287, 2010.

[9] A.M. Abbosh, "Ultra wideband balanced bandpass filter," *IEEE Microwave Wireless Components Lett*., vol. 21, 480–482, 2011

[10] B. Xia, L.-S. Wu, and J. F. Mao, "An ultra-wideband balanced bandpass filter based on defected ground structures," *Progress In Electromag. Research C*, vol. 25, 133-144, 2012

[11] Huang, J.-Q. and Q.-X. Chu, "Compact UWB band-pass filter utilizing modified composite right/left-handed structure with cross coupling," *Progress In Electromag. Research*, vol. 107, pp. 179-186, 2010.

[12] Tang, C.-W., and Chen, M.-G., "A microstrip ultra-wideband bandpass filter with cascaded broadband bandpass and bandstop filters," *IEEE Trans Microwave Theory Tech*, vol. 55, pp. 2412-2418, 2007

[13] Zhang, Z., and Xiao, F., "An UWB bandpass filter based on a novel type of multi-mode resonator," *IEEE Microwave Wireless Compon Lett*, vol. 22, 506–508, 2012

 © 2017 SBMO/SBMag